

1 **Effect of non-thermal plasma in the activation and regeneration of 13X zeolite for enhanced**
2 **VOC elimination by *cycled storage and discharge* process**

3
4 Savita Kaliya Perumal Veerapandian¹, Nathalie De Geyter¹, Jean-Marc Giraudon², Jean-Charles
5 Morin², Parinaz Saadat Esbah Tabaei¹, Guy De Weireld³, Andreas Laemont⁴, Karen Leus⁴, Pascal Van
6 Der Voort⁴, Jean-François Lamonier² and Rino Morent¹

7 ¹ *Ghent University, Faculty of Engineering and Architecture, Department of Applied Physics,*
8 *Research Unit Plasma Technology, Sint-Pietersnieuwstraat 41 B4, 9000 Ghent, Belgium*
9 *(*email: savita.kaliyaperumalveerapandian@ugent.be)*

10 ² *Univ. Lille, CNRS, Centrale Lille, Univ. Artois, UMR 8181 – UCCS – Unité de Catalyse et Chimie*
11 *du Solide, F-59000 Lille, France*

12 ³ *Université de Mons, Faculté Polytechnique, Service de Thermodynamique et de Physique*
13 *Mathématique, place du Parc, 20, 7000 Mons, Belgium*

14 ⁴ *Ghent University, Department of Chemistry, COMOC-Center for Ordered Materials,*
15 *Organometallics and Catalysis, Krijgslaan 281-S3, 9000 Ghent, Belgium*

16
17
18
19
20
21
22
23
24
25
26

271.1 Experimental set-up

28 The gas supply system consisted of two separate gas lines, each controlled by a mass flow controller
29 (MFC, El-flow®, Bronkhorst) to produce the feed gas of toluene diluted in dry air. The temperature and
30 humidity of the feed gas was monitored using a humidity measuring instrument (Testo 645). The
31 pressure drop in the packed DBD reactor and in the bypass was monitored using a pressure indicator
32 (DPI 705, Druck) and was kept constant using a pressure reducer (Swagelok).

33 The packed bed DBD reactor consisted of a quartz glass tube with a stainless-steel rod (diameter
34 0.4 cm) placed coaxially inside the tube, acting as high voltage electrode. The inner diameter, outer
35 diameter and wall thickness of the quartz glass tube were 1.6 cm, 2.2 cm and 0.3 cm, respectively. The
36 discharge length was maintained at 9 cm by using a stainless-steel mesh around the quartz tube which
37 acted as grounded electrode. The discharge gap was filled with 2 g of MS-13X (Alfa Aesar), which is
38 cylindrical in shape (length = 2.5 mm and diameter = 1.5 mm), and 25 g of round borosilicate glass
39 beads (Sigma-Aldrich) of 3 mm diameter on both sides of the MS-13X pellets, as shown in Figure S2.
40 An AC power supply with an operating frequency of 50 kHz, which was connected to the inner electrode,
41 powered the packed DBD reactor. The calculation of the discharge power $P_{discharge}$ (W) is explained
42 in detail elsewhere [9,25] and was determined using the following formula:

$$43 \quad P_{discharge} = f \int_0^t V(t)I(t)dt \quad 1$$

44 where $V(t)$ and $I(t)$ are the instantaneous voltage and current waveforms and f is the frequency of the
45 discharge.

46 The flue gas composition during different stages of the experiment was investigated in-line with
47 an FTIR spectrometer (Bruker, Tensor 27). The Tensor 27 FTIR was equipped with a DTGS (deuterated
48 triglycine sulfate) detector and a gas cell with a 20 cm optical path length fitted with ZnSe windows.
49 After reaching steady state conditions, FTIR spectra averaged over 20 samples were obtained with a
50 resolution of 4 cm^{-1} and an aperture of 6 mm. OPUS (Bruker) software was used to collect and analyse
51 the obtained FTIR spectra. The concentrations of toluene CO and CO₂ were obtained after FTIR
52 calibration using standard gas mixtures. On the other hand, other by-products such as NO, NO₂ and N₂O
53 were quantified using a more advanced FTIR spectrometer (Bruker, Matrix-MG2). The Matrix-MG2

54 FTIR was equipped with an IRCube module fitted with an MCT (mercury-cadmium-tellurium) detector
55 and a gas cell with a path length of 5 m. The optical compartment of the IRCube was sealed against the
56 gas cell using ZnSe windows. The gas cell was heated up to 191°C and the inlet gas tube up to 50°C to
57 avoid gas condensation. FTIR spectra averaged over 50 samples were obtained with a resolution of 1
58 cm⁻¹. The peak positions used for the identification of the by-products and the wavenumber range used
59 for the integration of the area under the peak for both qualitative and quantitative comparison are given
60 in Table S1.

61

621.2 Cycled storage and discharge process

63 The total amount of toluene adsorbed on MS-13X (mol/g) was quantified from the toluene
64 breakthrough curves using the following equation:

$$65 \quad [Toluene]_{adsorbed} = \int_0^{t_1} \frac{(C_0 - C) \times f_1 \times dt_1}{24.4 \times m} \times 10^{-6} \quad 2$$

66 where C_0 is the initial toluene concentration (ppm), C is the concentration of toluene in the outlet of the
67 NTP reactor (ppm), f_1 is the dry air flow rate during adsorption (L/min), t_1 is the adsorption time (mins),
68 and m is the mass of the MS-13X pellets packed in the DBD reactor (g).

69 The amount of toluene desorbed by flushing dry air (reversibly adsorbed toluene) and by
70 switching on the NTP (unconverted toluene) (mol/g) was calculated using the following equation:

$$71 \quad [Toluene]_{desorbed} = \int_0^{t_2} \frac{C_{Toluene} \times f_2 \times dt_2}{24.4 \times m} \times 10^{-6} \quad 3$$

72 where $C_{Toluene}$ is the concentration of desorbed toluene by flushing dry air or by switching on the
73 discharge (ppm), f_2 is the dry air flow rate used during flushing or NTP exposure (L/min), and t_2 is the
74 flushing time or the NTP exposure time (mins).

75 The amount of toluene irreversibly adsorbed after flushing by dry air was calculated by
76 $[Toluene]_{irreversible} = [Toluene]_{adsorbed} - [Toluene]_{desorbed \text{ by air}}$. The amount of toluene
77 converted by NTP exposure was calculated by $[Toluene]_{converted} = [Toluene]_{irreversible} -$
78 $[Toluene]_{desorbed \text{ by NTP}}$.

79 The amount of CO₂ and CO (mol/g) formed during NTP exposure were calculated using the
80 following equations:

$$81 \quad [CO_2]_{produced \text{ or } desorbed} = \int_0^{t_2} \frac{C_{CO_2} \times f_2 \times dt_2}{24.4 \times m} \times 10^{-6} \quad 4$$

$$82 \quad [CO]_{produced} = \int_0^{t_2} \frac{C_{CO} \times f_2 \times dt_2}{24.4 \times m} \times 10^{-6} \quad 5$$

83 where C_{CO_2} and C_{CO} are the concentrations of CO_2 and CO produced during NTP exposure (ppm),
 84 respectively, f_2 is the dry air flow rate during NTP exposure (L/min), and t_2 is the NTP exposure time
 85 (mins).

86 The CO_x selectivity, S_{CO_x} (%) and CO_x yield, Y_{CO_x} (%) were defined as follows:

$$87 \quad S_{CO_x} = \frac{C_{CO_x}}{7[C_{Toluene}]_{conv}} \times 100 \quad 6$$

$$88 \quad Y_{CO_x} = \frac{C_{CO_x}}{7[C_{Toluene}]_{ads}} \times 100 \quad 7$$

89 where $C_{CO_x} = C_{CO_2} + C_{CO}$ and C_{CO_2} and C_{CO} are the concentrations of CO_2 and CO produced during
 90 NTP exposure. Finally, in this study, the energy cost E_c (kWh/m³), which is the energy required to
 91 remedy 1 m³ of air using the sequential process and the energy yield E_y (g/kWh), which measures the
 92 energy efficiency of the [cycled storage and discharge](#) process were calculated using the following
 93 equations:

$$94 \quad E_c = \frac{P_{discharge}}{f_1} \times \frac{t_2}{t_1} \quad 8$$

$$95 \quad E_y = \frac{[Toluene]_{total \ adsorbed} \times 92.14 \times 60}{P_{discharge} \times t_2} \quad 9$$

96 where f_1 is the dry air flow rate (m³/h) during adsorption, and t_1 and t_2 are the adsorption and NTP
 97 exposure periods (mins), respectively.

98

991.3 Catalyst characterization

100 First of all, powder X-ray diffraction (PXRD) patterns of MS-13X were collected using a Thermo
 101 Scientific ARL X'Tra diffractometer, operating at 40 kV, 30 mA using Cu-K α radiation ($\lambda = 1.5406 \text{ \AA}$).
 102 The PXRD patterns were recorded over the range $3^\circ < 2\theta < 55^\circ$ using a step size of 0.02° and a scan rate
 103 of $0.5^\circ/\text{min}$.

104 X-ray photoelectron spectroscopy (XPS) survey spectra and high resolution C1s, O1s, Al2p, Si2p
 105 and Na1s XPS spectra of different MS-13X samples were obtained using a PHI Versaprobe II XPS

106 spectrometer equipped with a monochromatic Al K_α X-ray source (hν = 1486.6 eV) operating with a
107 beam size of 200 μm and a power of 50 W. The XPS measurements were conducted at a pressure of at
108 least 10⁻⁶ Pa and the photoelectrons were detected by a hemispherical analyser positioned at an angle of
109 45° with respect to the normal of the sample surface. Moreover, X-ray induced secondary electron
110 images (SXIs) of the sample were obtained by scanning a finely focused X-ray beam characterized by
111 a sub-10 μm size across the surface. Such images are used to navigate the features of interest on the
112 sample and precisely select the spot locations for analysis. The pass energies used for acquiring the
113 survey and individual high resolution XPS spectra were 187.85 eV and 23.5 eV, respectively. The
114 surface atomic elemental composition of the samples was calculated from XPS survey spectra using
115 Multipak software. For this purpose, the adventitious carbon at 285 eV was used as internal standard
116 and an iterated Shirley background was applied to determine the elemental composition. In addition, the
117 deconvolution of the high resolution XPS spectra was also carried out in this study. To do so, Gaussian-
118 Lorentzian peak shapes (80–100% Gaussian) were employed and a full width at half maximum (FWHM)
119 set between 1.4 eV and 1.6 eV was adopted for each line shape dye.

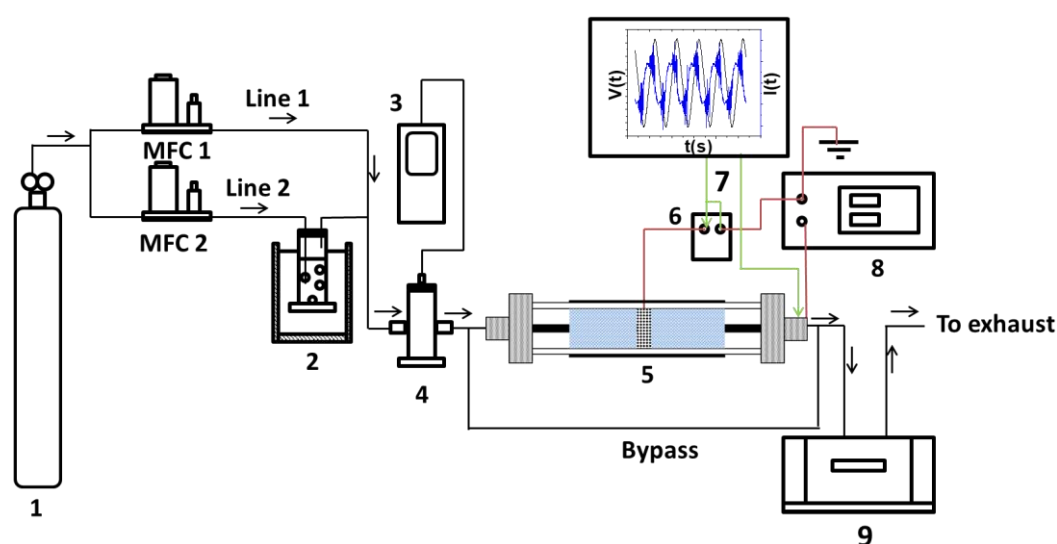
120 Nitrogen adsorption-desorption measurements at the temperature of liquid nitrogen (-196°C) were
121 performed to analyse the specific surface area, pore volume and pore size distribution of the zeolites
122 using a Micromeritics Tristar II 3020 device. Prior to the measurements, the MS-13X samples were
123 degassed at 120°C overnight. The specific surface area and pore volume were determined using the
124 Brunauer-Emmett-Teller (BET) method. In addition, argon sorption measurements were also recorded
125 at -186°C to study, in particular, the distribution of the micropores using a Quantachrome Autosorb-1-
126 MP automated gas sorption system. Prior to the measurements, the samples were degassed for 24 h
127 under high vacuum at a temperature of 150°C.

128 Finally, the acidic properties of the MS-13X samples were determined by means of FTIR
129 spectroscopy of chemisorbed pyridine (py-FTIR) using a Thermo Nicolet 460 Protegé spectrometer
130 equipped with an MCT detector. Prior to FTIR analysis, the MS-13X samples were pressed to form self-
131 supporting discs (6-8 mg/cm²) and activated at 400°C overnight under high vacuum (< 10⁻⁷ mbar).
132 Afterwards, the activated samples were saturated with pyridine vapour at 1.2 mbar for 30 minutes at
133 100°C. In a next step, the desorption of pyridine under high vacuum was performed at different

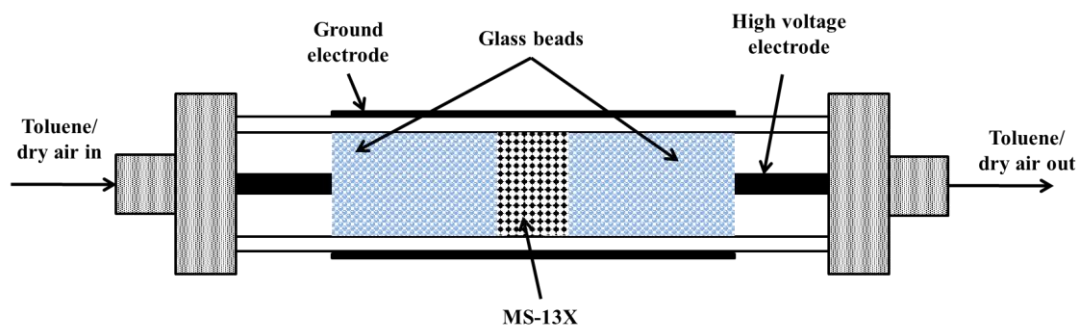
134 temperatures (150°C, 250°C, 350°C and 450°C) and FTIR spectra averaged over 256 scans were
135 recorded simultaneously with a resolution of 2 cm⁻¹. The surface concentration of the Brønsted and
136 Lewis acid sites was calculated using the following formula:

$$137 \quad n = \frac{A \times s}{\epsilon \times m} \quad 10$$

138 where n is the surface acidic site concentration (μmol/g), A is the integrated area under the absorbance
139 band corresponding to pyridine adsorption (cm⁻¹) on Brønsted acid sites (1545 cm⁻¹) or Lewis acid sites
140 (1445 cm⁻¹), s is the area of the pressed sample (cm²), ϵ is the pyridine molar extinction coefficient (1.67
141 cm/μmol for Brønsted acid sites and 2.22 cm/μmol for Lewis acid sites) and m is the mass of the pressed
142 sample (g).

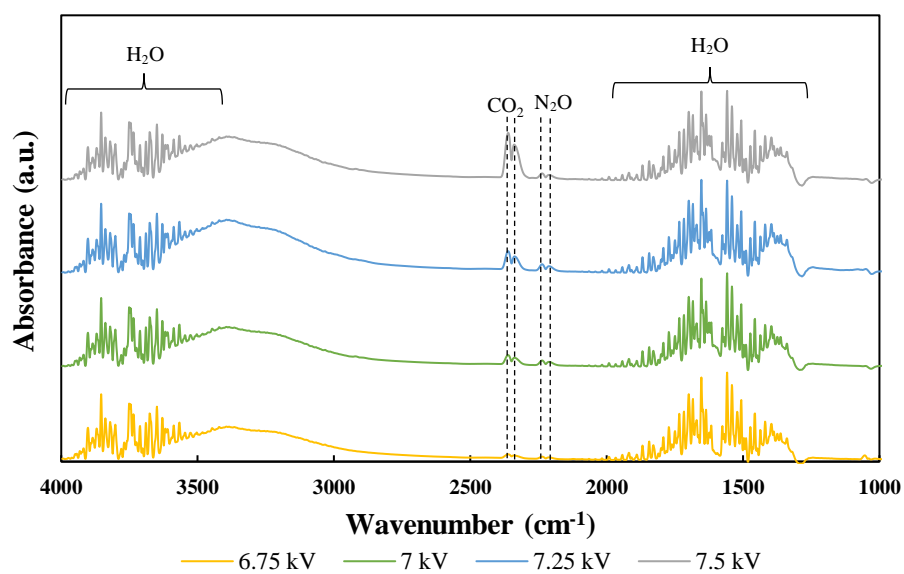


143
144 *Figure S1 Schematic representation of the experimental set-up used for the **cycled storage and discharge***
145 ***process** of toluene **removal**: 1-dry air cylinder, 2-toluene bubbler, 3-humidity meter, 4-mixing chamber,*
146 *5-MS-13X/glass beads DBD reactor, 6-resistor (46.4 Ω), 7-high voltage and current probe, 8-AC power*
147 *supply (50 kHz), 9-FTIR spectrometer*
148



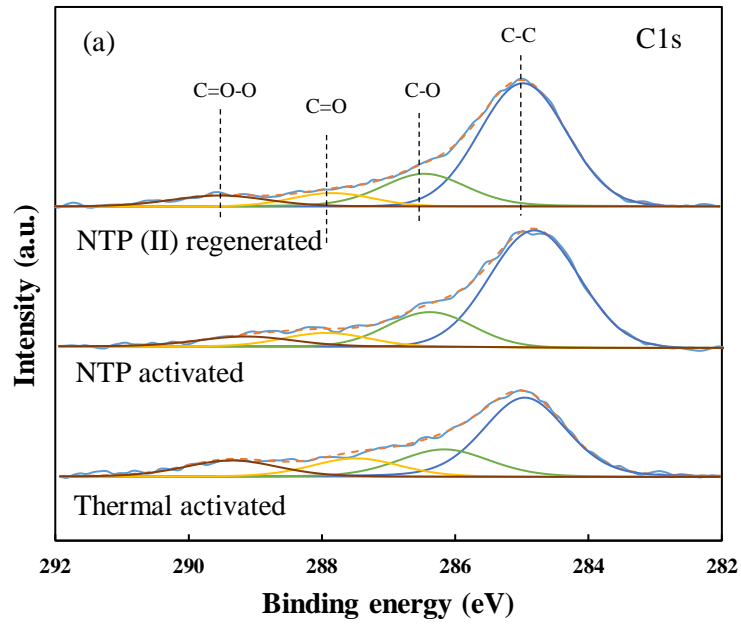
149

150 *Figure S2 Schematic representation of the MS-13X pellets & glass beads packed bed DBD reactor*

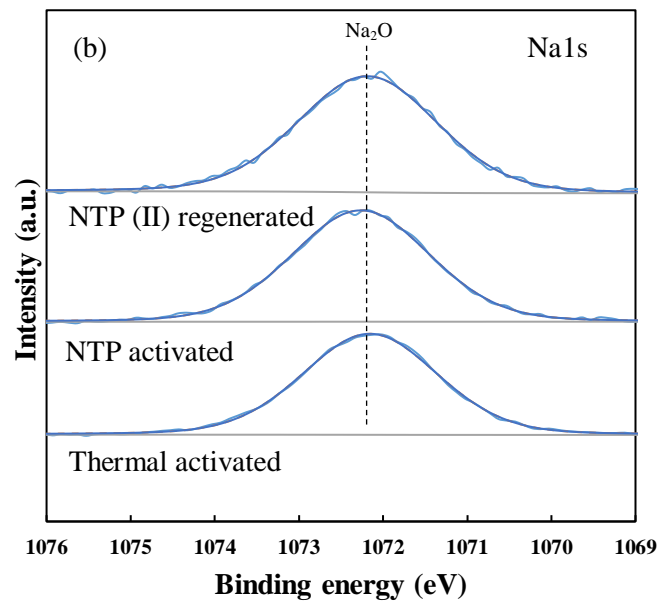


151

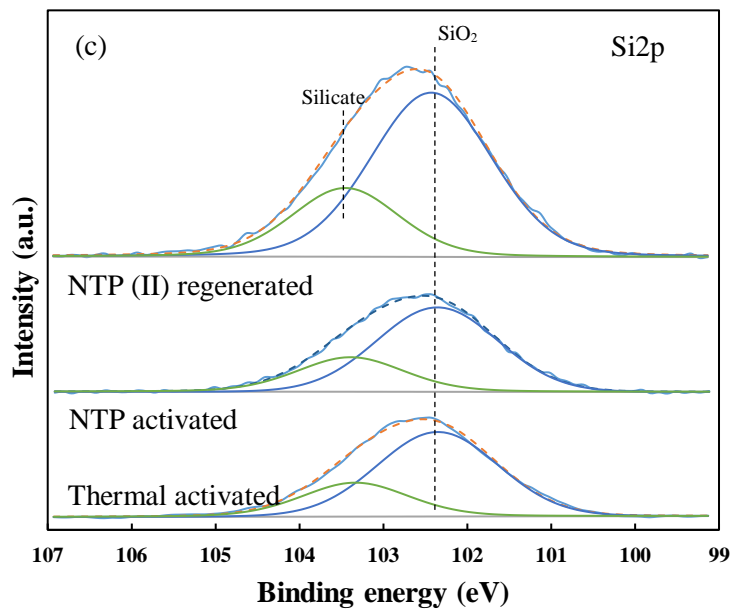
152 *Figure S3 FTIR spectra of the outlet gas after 10 minutes of NTP activation using different applied*
 153 *voltages (dry air flow rate=0.5 L/min)*



154



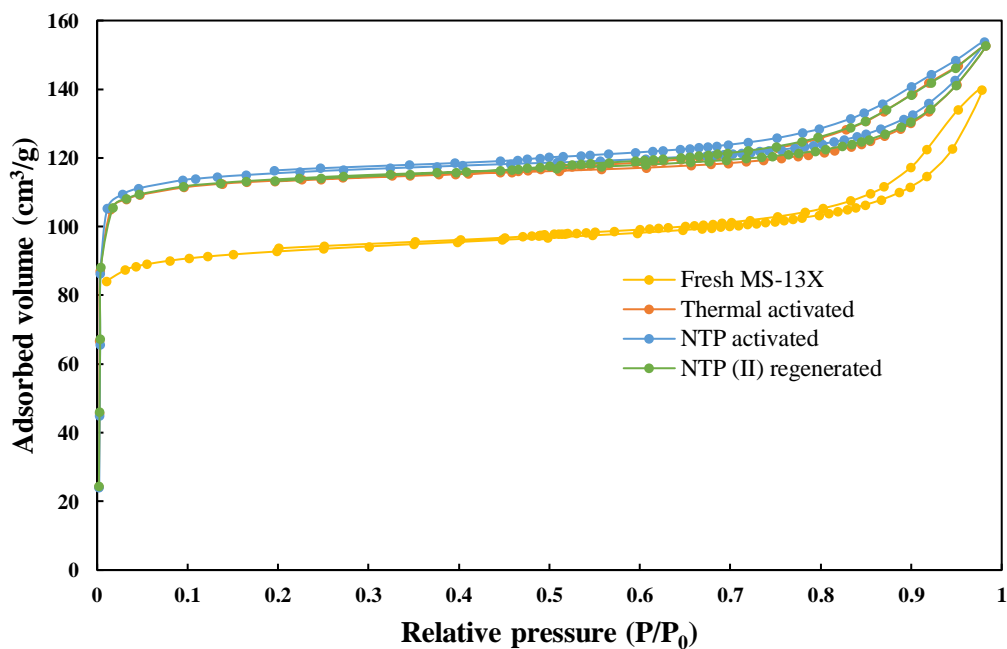
155



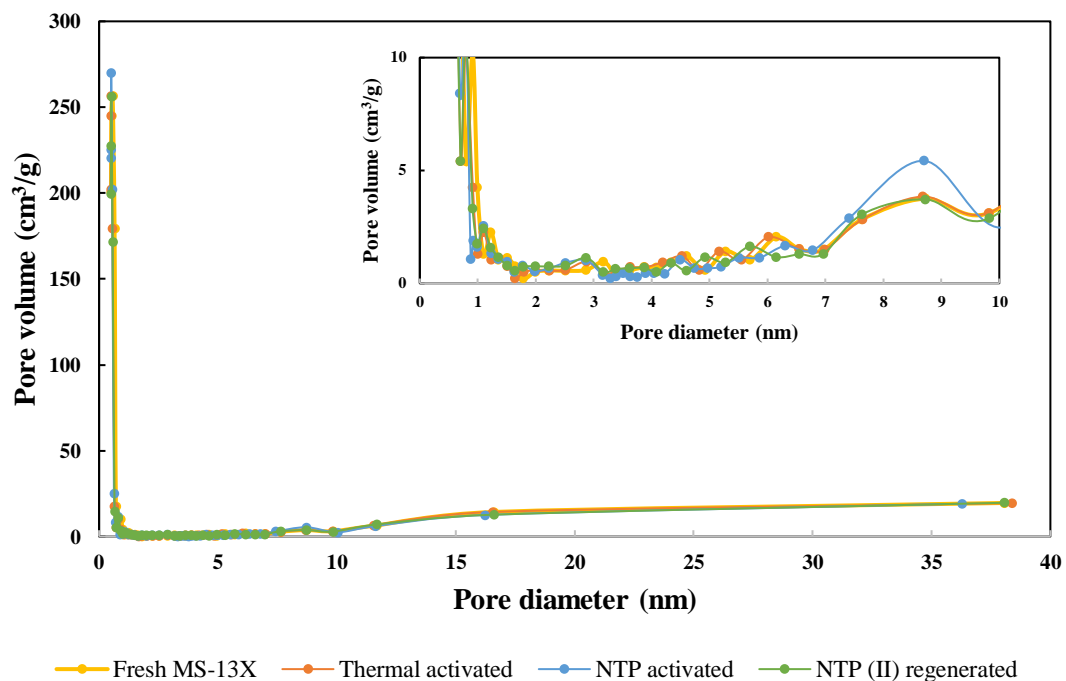
156

157 Figure S4 XPS high-resolution spectra of (a) C1s, (b) Na1s and (c) Si2p for thermal activated, NTP
 158 activated and NTP (II) regenerated MS-13X

159



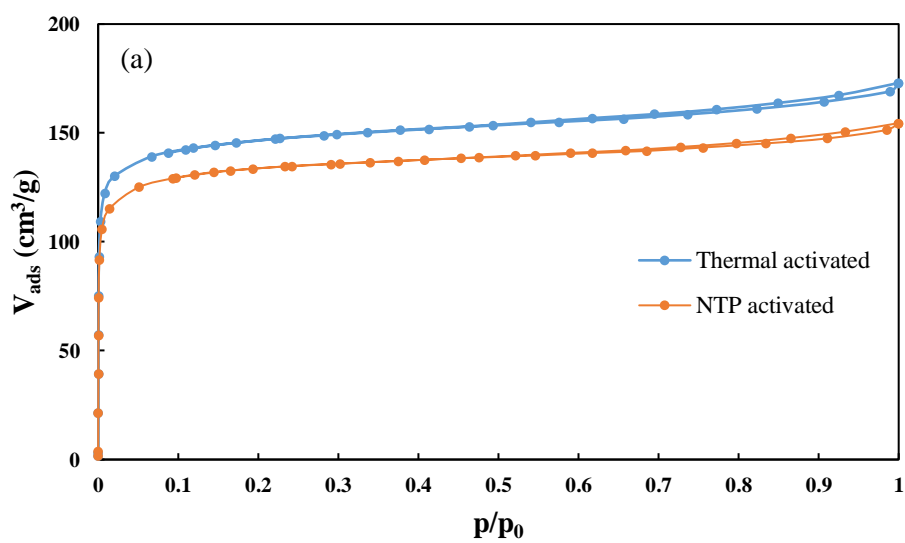
160



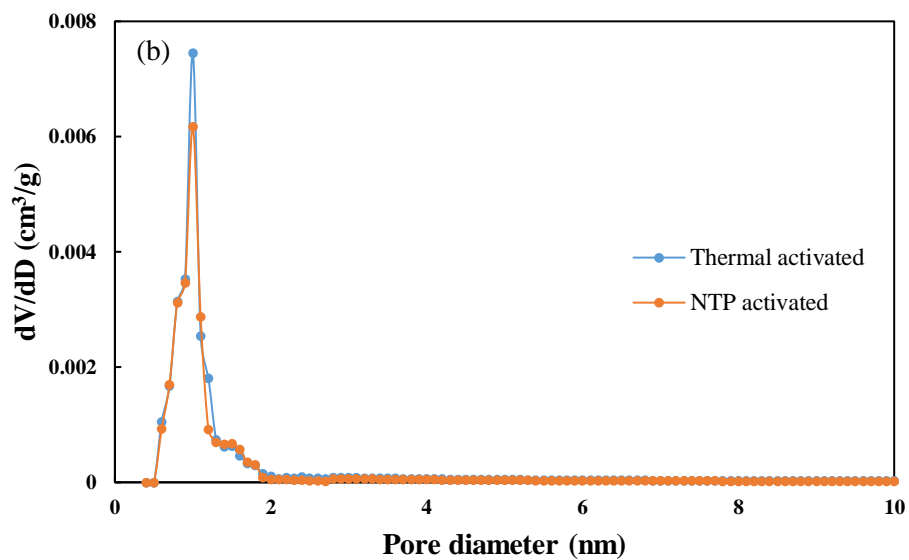
161

162 *Figure S5 (a) Nitrogen adsorption-desorption isotherms and (b) BJH pore size distribution for fresh,*

163 *thermal activated, NTP activated and NTP (II) regenerated MS-13X*



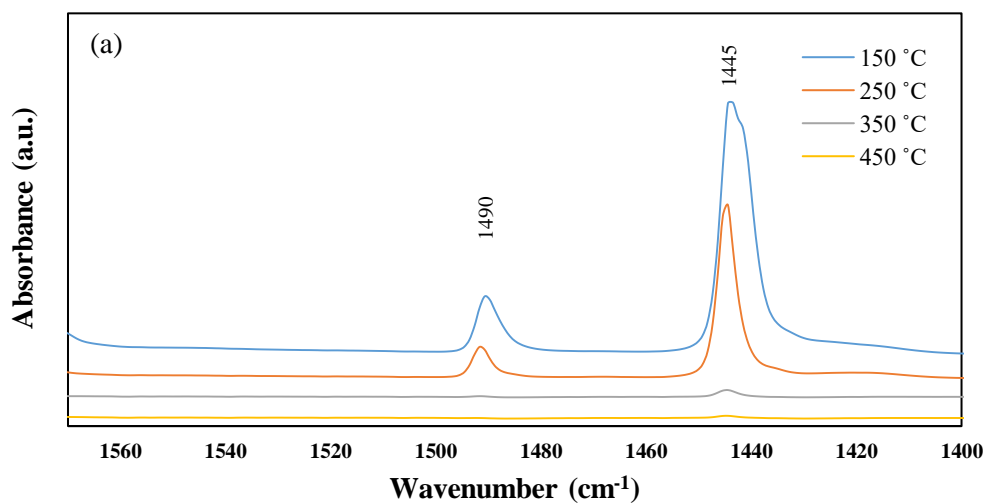
164



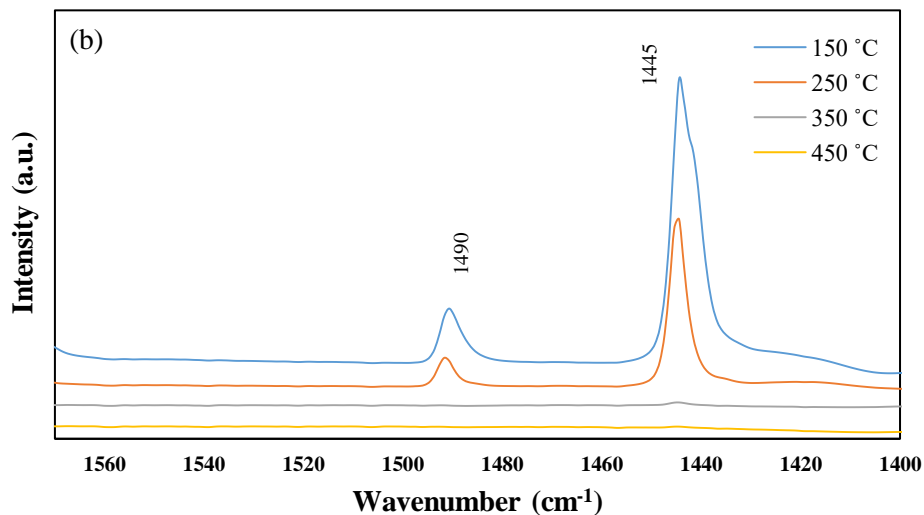
165

166 *Figure S6 (a) Ar adsorption isotherms and pore size distribution obtained from Ar sorption for thermal*

167 *and NTP activated MS-13X*



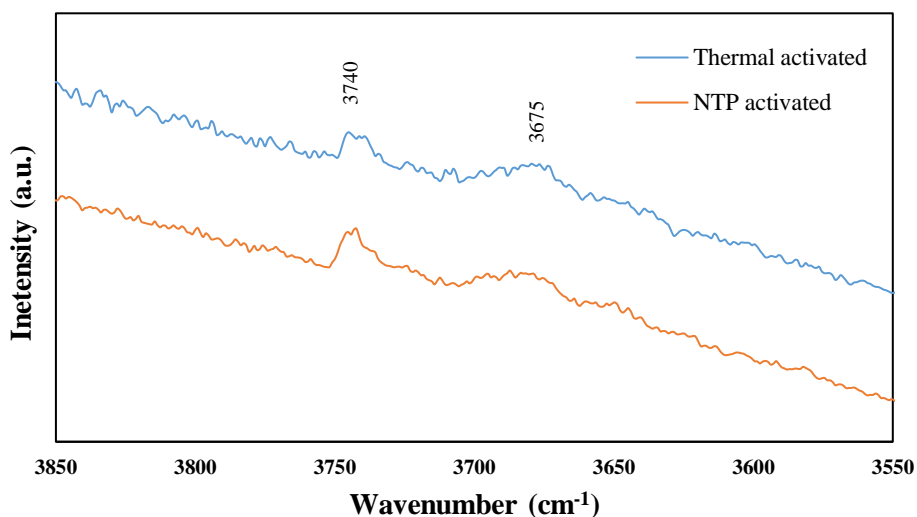
168



169

170 *Figure S7 Subtracted FTIR spectra in the region 1570 – 1400 cm⁻¹ obtained after desorption of pyridine*

171 *at different temperatures for (a) thermal activated and (b) NTP activated MS-13X*

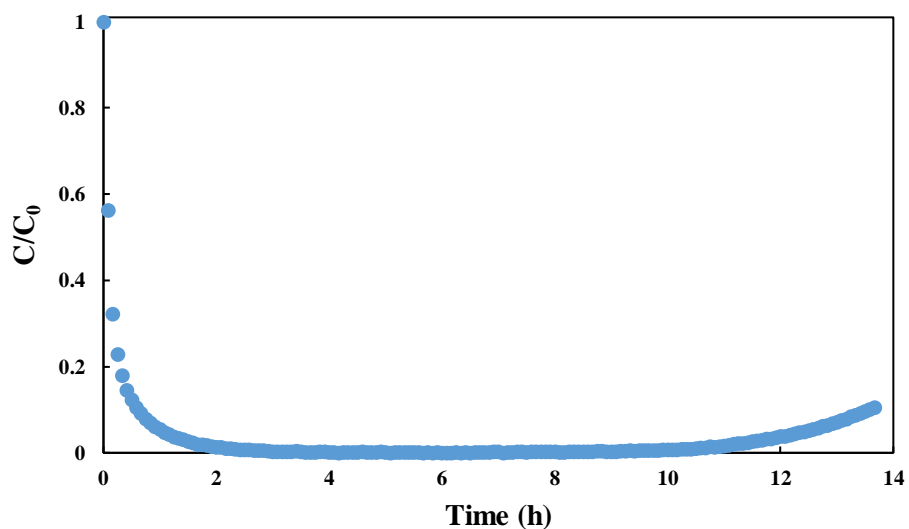


172

173 *Figure S8 Reprocessed FTIR spectra in the region 3850 - 3550 cm⁻¹ obtained after desorption of pyridine*

174 *at 450 °C for (a) thermal activated and (b) NTP activated MS-13X*

175



176

177 *Figure S9 Breakthrough curve for the adsorption of toluene from dry air until the concentration in the*
 178 *outlet reaches a critical concentration (10% of the initial concentration) on NTP activated MS-13X*
 179 *pellets (flow rate=0.1 L/min; toluene initial concentration=1000 ppm)*

180

181

Table S1 Parameters used for flue gas analysis using FTIR

Compound	Peak position (cm⁻¹)	Wavenumber range (cm⁻¹)
Toluene	3074, 3038, 2938, 2882, 1610, 1500, 729, 694	3059-3010
CO	2175, 2120	2143-2030
CO₂	3729, 3703, 3627, 3599, 2360, 2341	2394-2283
H₂O	--	1881-1353
O₃	2108, 1055, 1032	1070-1044
N₂O	2236, 2211	2260-2223
NO	1903, 1845	1929-1883
NO₂	2918, 2894, 1628, 1601	1655-1574

182

183 *Table S2 Experimental parameters used during the different steps of the **cycled storage and discharge***
 184 *process for the abatement of toluene in dry air using a MS-13X pellets & glass beads packed DBD*
 185 *reactor*

Plasma activation	
Gas source	Dry air
Flow rate	0.5 L/min
Applied voltage	7.25 kV
Discharge power	58 W
Treatment time	60 mins
Toluene adsorption	
Gas source	Dry air
Flow rate	0.1 L/min
Inlet toluene concentration	1000 ± 10 ppm
Toluene desorption by air	
Gas source	Dry air
Flow rate	0.5 L/min
Temperature	RT (=18 °C)
NTP exposure (for oxidation and regeneration)	
Gas source	Dry air
Flow rate	0.5 L/min
Applied voltage	7.5 kV
Discharge power	65 W
Treatment time	70 mins

186

187

188

189

190 *Table S3 Amount of toluene adsorbed and desorbed, CO₂, CO and CO_x formation during NTP*
 191 *exposure for NTP activated and NTP(I) regenerated MS-13X*

	NTP activated	NTP (I) regenerated
	MS-13X	
Total adsorbed toluene (mmol/g)	2.45 ± 0.06	2.49 ± 0.03
Toluene desorbed by flushing dry air (reversibly adsorbed toluene) (mmol/g)	0.12	0.12
Irreversibly adsorbed toluene (mmol/g)	2.33 ± 0.05	2.37 ± 0.03
Toluene desorbed by NTP exposure (unconverted toluene) (mmol/g)	1.04	1.09
Converted toluene by NTP exposure (mmol/g)	1.29 ± 0.03	1.28 ± 0.01
CO ₂ formation (mmol/g)	1.90	1.66
CO formation (mmol/g)	0.72	0.64
CO _x formation (mmol/g)	2.62	2.30

192

193

194

195

196 *Table S4 The total amount of toluene adsorbed on MS-13X pellets (until the critical concentration),*
 197 *the regeneration efficiency, and the CO₂ and CO_x selectivity during NTP exposure for different cycles*
 198 *of cycled storage and discharge process for the abatement of toluene*

Cycle No.	Adsorbed toluene (mmol/g)	Regeneration efficiency (%)	CO ₂ selectivity (%)	CO _x selectivity (%)
1	1.84 ± 0.01	NA	26.0 ± 0.1	35.9 ± 0.1
2	1.83 ± 0.01	99	25.8 ± 0.1	35.9 ± 0.1
3	1.79 ± 0.01	97	25.7 ± 0.1	35.8 ± 0.1
4	1.78 ± 0.01	97	26.0 ± 0.1	36.1 ± 0.1
5	1.84 ± 0.01	100	24.1 ± 0.0	33.5 ± 0.1
6	1.86 ± 0.01	101	25.5 ± 0.1	35.3 ± 0.1
7	1.89 ± 0.01	103	25.6 ± 0.1	34.1 ± 0.1
8	1.90 ± 0.01	103	23.9 ± 0.0	33.2 ± 0.1
9	1.79 ± 0.01	97	26.1 ± 0.1	36.3 ± 0.2
10	1.78 ± 0.01	97	27.2 ± 0.0	37.9 ± 0.1

199

200